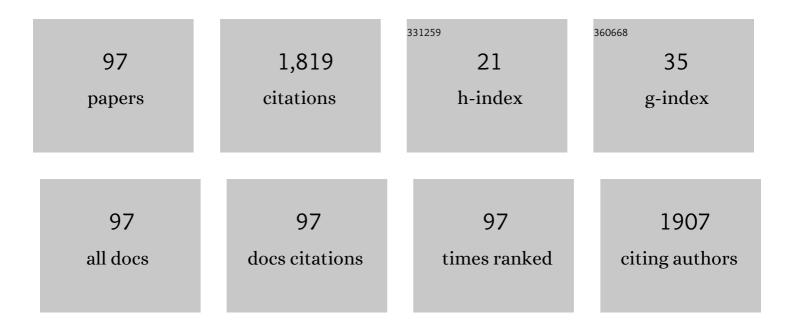
Qiwu Shi

List of Publications by Year in descending order

Source: https://exaly.com/author-pdf/4682390/publications.pdf Version: 2024-02-01



#	Article	IF	CITATIONS
1	Dynamic Photoinduced Controlling of the Large Phase Shift of Terahertz Waves via Vanadium Dioxide Coupling Nanostructures. ACS Photonics, 2018, 5, 3040-3050.	3.2	111
2	Giant Phase Transition Properties at Terahertz Range in VO ₂ films Deposited by Sol–Gel Method. ACS Applied Materials & Interfaces, 2011, 3, 3523-3527.	4.0	92
3	One-Step Hydrothermal Synthesis of W-Doped VO ₂ (M) Nanorods with a Tunable Phase-Transition Temperature for Infrared Smart Windows. ACS Omega, 2016, 1, 1139-1148.	1.6	76
4	Effect of annealing temperature on thermochromic properties of vanadium dioxide thin films deposited by organic sol–gel method. Applied Surface Science, 2013, 268, 556-560.	3.1	68
5	A CTAB-assisted hydrothermal synthesis of VO 2 (B) nanostructures for lithium-ion battery application. Ceramics International, 2013, 39, 6199-6206.	2.3	62
6	Sol–gel fabrication of WO ₃ /RGO nanocomposite film with enhanced electrochromic performance. RSC Advances, 2016, 6, 67488-67494.	1.7	58
7	THz medical imaging: from in vitro to in vivo. Trends in Biotechnology, 2022, 40, 816-830.	4.9	56
8	Near-perfect terahertz wave amplitude modulation enabled by impedance matching in VO2 thin films. Applied Physics Letters, 2018, 112, .	1.5	55
9	Synthesis and properties of Mo and W ions co-doped porous nano-structured VO2 films by sol–gel process. Journal of Sol-Gel Science and Technology, 2012, 64, 493-499.	1.1	47
10	Preparation and thermochromic properties of Ce-doped VO2 films. Materials Research Bulletin, 2013, 48, 2268-2271.	2.7	38
11	Terahertz transmission characteristics across the phase transition in VO2 films deposited on Si, sapphire, and SiO2 substrates. Journal of Applied Physics, 2012, 112, .	1.1	35
12	Preparation and characterization of λ-Ti3O5 by carbothermal reduction of TiO2. Journal of Alloys and Compounds, 2015, 621, 404-410.	2.8	32
13	Fabrication of nanostructured Li 2 TiO 3 ceramic pebbles as tritium breeders using powder particles synthesised via a CTAB-assisted method. Ceramics International, 2017, 43, 5680-5686.	2.3	31
14	Preparation and phase transition characterization of VO2 thin film on single crystal Si (100) substrate by sol–gel process. Journal of Sol-Gel Science and Technology, 2011, 59, 591-597.	1.1	28
15	A promising tritium breeding material: Nanostructured 2Li2TiO3-Li4SiO4 biphasic ceramic pebbles. Journal of Nuclear Materials, 2018, 500, 265-269.	1.3	28
16	Gasâ€Phase and Solid‣tate Simultaneous Mechanism for Two‣tep Carbothermal AlON Formation. Journal of the American Ceramic Society, 2015, 98, 1965-1973.	1.9	26
17	Stabilization of microcrystal λ-Ti3O5 at room temperature by aluminum-ion doping. Applied Physics Letters, 2017, 111, .	1.5	25
18	A facile solvothermal method for high-quality Gd2Zr2O7 nanopowder preparation. Ceramics International, 2018, 44, 1334-1342.	2.3	25

#	Article	IF	CITATIONS
19	The role of lattice dynamics in ferroelectric switching. Nature Communications, 2022, 13, 1110.	5.8	25
20	Fabrication of nanocrystalline λ-Ti ₃ O ₅ with tunable terahertz wave transmission properties across a temperature induced phase transition. Journal of Materials Chemistry C, 2016, 4, 10279-10285.	2.7	24
21	Preparation and phase transition properties of Ti-doped VO2 films by sol–gel process. Journal of Sol-Gel Science and Technology, 2016, 78, 19-25.	1.1	23
22	Nanostructured VO2 film with high transparency and enhanced switching ratio in THz range. Applied Physics Letters, 2014, 104, .	1.5	22
23	Thermal stability of VO2 thin films deposited by sol–gel method. Journal of Sol-Gel Science and Technology, 2015, 75, 189-197.	1.1	22
24	Microstructure and phase evolution of Li4TiO4 ceramics pebbles prepared from a nanostructured precursor powder synthesized by hydrothermal method. Journal of Nuclear Materials, 2018, 508, 434-439.	1.3	22
25	Phase evolution and formation of $\hat{\sf l} ^{\sf v}$ phase in Ti3O5 induced by magnesium doping. Journal of Alloys and Compounds, 2019, 774, 1189-1194.	2.8	22
26	Curing of polyester powder coating modified with rutile nano-sized titanium dioxide studied by DSC and real-time FT-IR. Journal of Thermal Analysis and Calorimetry, 2012, 108, 1243-1249.	2.0	21
27	Flexible and Giant Terahertz Modulation Based on Ultra-Strain-Sensitive Conductive Polymer Composites. ACS Applied Materials & Interfaces, 2020, 12, 9790-9796.	4.0	21
28	Low temperature fabrication of hydrangea-like NiCo2S4 as electrode materials for high performance supercapacitors. Materials Letters, 2017, 186, 206-209.	1.3	20
29	Enhanced Electrochromic Performance of Mesoporous Titanium Dioxide/Reduced Graphene Oxide Nanocomposite Film Prepared by Electrophoresis Deposition. Journal of the Electrochemical Society, 2018, 165, H804-H812.	1.3	19
30	Terahertz Switchable Focusing Planar Lens With a Nanoscale Vanadium Dioxide Integrated Metasurface. IEEE Transactions on Terahertz Science and Technology, 2022, 12, 13-22.	2.0	19
31	Effects of porous nano-structure on the metal–insulator transition in VO2 films. Applied Surface Science, 2012, 259, 256-260.	3.1	18
32	Preparation and ageing-resistant properties of polyester composites modified with functional nanoscale additives. Nanoscale Research Letters, 2014, 9, 215.	3.1	18
33	Fabrication of attractive Li 4 SiO 4 pebbles with modified powders synthesized via surfactant-assisted hydrothermal method. Ceramics International, 2016, 42, 10014-10020.	2.3	18
34	Flexible reduced graphene oxide paper with excellent electromagnetic interference shielding for terahertz wave. Journal of Materials Science: Materials in Electronics, 2018, 29, 17245-17253.	1.1	18
35	On-Chip THz Dynamic Manipulation Based on Tunable Spoof Surface Plasmon Polaritons. IEEE Electron Device Letters, 2019, 40, 1844-1847.	2.2	18
36	Synthesis of CoV2O6/CNTs composites via ultrasound as electrode materials for supercapacitors. Journal of Materials Science: Materials in Electronics, 2020, 31, 2388-2397.	1.1	18

#	Article	IF	CITATIONS
37	Hollow structured black TiO2 with thickness-controllable microporous shells for enhanced visible-light-driven photocatalysis. Microporous and Mesoporous Materials, 2021, 323, 111228.	2.2	18
38	Fast fabrication of high quality Li2TiO3–Li4SiO4 biphasic ceramic pebbles by microwave sintering: In comparison with conventional sintering. Ceramics International, 2019, 45, 19022-19026.	2.3	17
39	A novel mass production method for Li2TiO3 tritium breeder ceramic pebbles using polyvinyl alcohol (PVA) and polyvinyl pyrrolidone (PVP) assisted granulation method. Ceramics International, 2020, 46, 4167-4173.	2.3	17
40	Reconfigurable Optical Physical Unclonable Functions Enabled by VO ₂ Nanocrystal Films. ACS Applied Materials & Interfaces, 2022, 14, 5785-5796.	4.0	17
41	Freeze-drying induced nanocrystallization of VO2 (M) with improved mid-infrared switching properties. Journal of Alloys and Compounds, 2017, 728, 1076-1082.	2.8	16
42	Porous nano-structured VO2 films with different surfactants: synthesis mechanisms, characterization, and applications. Journal of Materials Science: Materials in Electronics, 2013, 24, 3823-3829.	1.1	15
43	Fast crystallization of amorphous Gd2Zr2O7 induced by thermally activated electron-beam irradiation. Journal of Applied Physics, 2015, 118, 214901.	1.1	15
44	Enhanced Electrochromic Performance of Vanadium Pentoxide/Reduced Graphene Oxide Nanocomposite Film Prepared by the Sol–Gel Method. Journal of the Electrochemical Society, 2016, 163, H891-H895.	1.3	15
45	Mesoporous hollow black TiO ₂ with controlled lattice disorder degrees for highly efficient visible-light-driven photocatalysis. RSC Advances, 2019, 9, 36907-36914.	1.7	15
46	Improving water dispersibility of non-covalent functionalized reduced graphene oxide with l-tryptophan via cleaning oxidative debris. Journal of Materials Science: Materials in Electronics, 2016, 27, 7361-7368.	1.1	14
47	Effect of deposition time on the growth mode and stoichiometric of amorphous boron carbide thin films deposited by electron beam evaporation. Ceramics International, 2018, 44, 17298-17304.	2.3	14
48	Silica-Coated Gold Nanorods with High Photothermal Efficiency and Biocompatibility as a Contrast Agent for <i>In Vitro</i> Terahertz Imaging. Journal of Biomedical Nanotechnology, 2019, 15, 910-920.	0.5	14
49	Low-cost fabrication of Li2TiO3 tritium breeding ceramic pebbles via low-temperature solid-state precursor method. Ceramics International, 2019, 45, 17114-17119.	2.3	13
50	In-situ stirring assisted hydrothermal synthesis of W-doped VO2 (M) nanorods with improved doping efficiency and mid-infrared switching property. Journal of Alloys and Compounds, 2020, 821, 153556.	2.8	13
51	Preparation of Li4TiO4-Li2TiO3 core-shell ceramic pebbles with thick shells and high strength through an improved granulation method. Journal of Nuclear Materials, 2021, 543, 152580.	1.3	13
52	Optical-Transparent Self-Assembled MXene Film with High-Efficiency Terahertz Reflection Modulation. ACS Applied Materials & Interfaces, 2021, 13, 10574-10582.	4.0	13
53	Temperature dependence of charging characteristic of C-free Li2O2 cathode in Li-O2 battery. Journal of Solid State Electrochemistry, 2013, 17, 2061-2069.	1.2	12
54	Rapid preparation and uniformity control of B4C ceramic double-curvature shells: Aim to advance its applications as ICF capsules. Journal of Alloys and Compounds, 2018, 762, 67-72.	2.8	12

#	Article	IF	CITATIONS
55	A Phase Transition Oxide/Graphene Interface for Incidentâ€Angleâ€Agile, Ultrabroadband, and Deep THz Modulation. Advanced Materials Interfaces, 2020, 7, 2001297.	1.9	12
56	Giant impact of self-photothermal on light-induced ultrafast insulator-to-metal transition in VO ₂ nanofilms at terahertz frequency. Optics Express, 2018, 26, 28051.	1.7	12
57	VO2-metallic hybrid metasurfaces for agile terahertz wave modulation by phase transition. APL Materials, 2022, 10, .	2.2	12
58	Enhanced hydrophilicity of the Si substrate for deposition of VO2 film by sol–gel method. Journal of Materials Science: Materials in Electronics, 2012, 23, 1610-1615.	1.1	11
59	Shape-dependent thermochromic phenomenon in porous nano-structured VO2 films. Materials Research Bulletin, 2013, 48, 4146-4149.	2.7	11
60	Pressure Dependence of Electrical Conductivity of Black Titania Hydrogenated at Different Temperatures. Journal of Physical Chemistry C, 2019, 123, 4094-4102.	1.5	11
61	Synthesis, characterization and sintering of Li2TiO3 nanoparticles via low temperature solid-state reaction. Ceramics International, 2020, 46, 1816-1823.	2.3	11
62	Characterization of Li-rich Li2TiO3 ceramic pebbles prepared by rolling method sintered in air and vacuum. Journal of Nuclear Materials, 2021, 546, 152786.	1.3	11
63	Influence of helium ion radiation on the nano-grained Li2TiO3 ceramic for tritium breeding. Ceramics International, 2021, 47, 28357-28366.	2.3	11
64	Preparation of a B4C hollow microsphere through gel-casting for an inertial confinement fusion (ICF) target. Ceramics International, 2017, 43, 571-577.	2.3	10
65	Enhanced photoresponses of an optically driven VO2-based terahertz wave modulator near percolation threshold. Applied Physics Letters, 2018, 113, .	1.5	10
66	Transparent AlON ceramic combined with VO2 thin film for infrared and terahertz smart window. Ceramics International, 2018, 44, 13674-13680.	2.3	10
67	Tritium release behavior of Li4SiO4 and Li4SiO4Â+ 5Âmol% TiO2 ceramic pebbles with small grain size. Journal of Nuclear Materials, 2019, 514, 284-289.	1.3	10
68	Flexible VO2/Mica thin films with excellent phase transition properties fabricated by RF magnetron sputtering. Vacuum, 2021, 192, 110407.	1.6	10
69	Phase transition properties of vanadium oxide films deposited by polymer-assisted deposition. Journal of Sol-Gel Science and Technology, 2014, 72, 565-570.	1.1	9
70	Geometrical morphology optimisation of laser drilling in B4C ceramic: From plate to hollow microsphere. Ceramics International, 2018, 44, 1370-1375.	2.3	9
71	Improved chemical precipitation prepared rapidly NiCo2S4 with high specific capacitance for supercapacitors. Nanotechnology, 2021, 32, 085604.	1.3	9
72	Volatile and Nonvolatile Switching of Phase Change Material Ge ₂ Sb ₂ Te ₅ Revealed by Time-Resolved Terahertz Spectroscopy. Journal of Physical Chemistry Letters, 2022, 13, 947-953.	2.1	9

#	Article	IF	CITATIONS
73	Two-Channel VO2 Memory Meta-Device for Terahertz Waves. Nanomaterials, 2021, 11, 3409.	1.9	9
74	Photoluminescence enhancement of YAG:Ce nanophosphors with SiO2 additions. Journal of Materials Science: Materials in Electronics, 2015, 26, 2451-2456.	1.1	8
75	Development of an advanced core-shell ceramic pebble with Li4TiO4 pure phase core and Li2TiO3 nanostructured shell by a physical coating method. Journal of Nuclear Materials, 2019, 520, 252-257.	1.3	8
76	Effect of coating layers on nano-TiO2 particles on the preparation of nanocrystalline λ-Ti3O5 by carbonthermal reduction. Journal of Materials Science: Materials in Electronics, 2016, 27, 4216-4222.	1.1	7
77	Low-temperature preparation of nanostructured Li2TiO3 tritium breeder ceramic pebbles using CTAB-modified ultrafine powders byÂaÂmixed solvent-thermal method. Journal of Nuclear Materials, 2019, 519, 315-321.	1.3	7
78	Surface morphology and microstructure evolution of B4C ceramic hollow microspheres prepared by wet coating method on a pyrolysis substrate. Ceramics International, 2019, 45, 7916-7922.	2.3	7
79	An innovative process for synthesis of superfine nanostructured Li2TiO3 tritium breeder ceramic pebbles via TBOT hydrolysis – solvothermal method. Ceramics International, 2019, 45, 5189-5194.	2.3	7
80	Hydrothermal activated carbon cloth as electrode materials for symmetric supercapacitors. Ionics, 2020, 26, 1457-1464.	1.2	7
81	Characteristics of CeOx–VO2 composite thin films synthesized by sol–gel process. Journal of Materials Science: Materials in Electronics, 2013, 24, 3496-3503.	1.1	6
82	Low-temperature fabrication of Li2O porous ceramic pebbles by two-stage support decomposition. International Journal of Hydrogen Energy, 2019, 44, 20249-20256.	3.8	6
83	In situ growth of sol–gel-derived nano-VO2 film and its phase transition characteristics. Journal of Nanoparticle Research, 2014, 16, 1.	0.8	5
84	Photothermal conversion of Ti2O3 film for tuning terahertz waves. IScience, 2022, 25, 103661.	1.9	5
85	Synthesis of nanoscale lambda-Ti3O5 via a PEG assisted sol-gel method. Journal of Alloys and Compounds, 2020, 848, 156585.	2.8	4
86	Transcriptome profiling of cells exposed to particular and intense electromagnetic radiation emitted by the "SG-III" prototype laser facility. Scientific Reports, 2021, 11, 2017.	1.6	4
87	Synthesis of ultra-fine and controllable size distribution nanocrystalline MgAl2O4 powders and ascertainment of aluminum loss by introducing inert atmosphere pre-calcination during combustion. Journal of Sol-Gel Science and Technology, 2015, 75, 336-344.	1.1	3
88	High-frequency response in Sr1â^'xCaxTiO3 powders studied by terahertz time-domain spectroscopy. Journal of Materials Science: Materials in Electronics, 2016, 27, 6318-6324.	1.1	3
89	Preparation of VO2 films via microspacing in-air sublimation method. Vacuum, 2022, 200, 110996.	1.6	3
90	Characterization of cation disorder and oxygen vacancies in Liâ€rich Li ₂ TiO ₃ . Journal of the American Ceramic Society, 2022, 105, 6407-6416.	1.9	3

Qıwu Sнı

#	Article	IF	CITATIONS
91	Highly efficient preparation of Li 2 O breeder materials with coreâ€shell structure by oilâ€based granulation route. Journal of the American Ceramic Society, 2020, 103, 5612-5623.	1.9	2
92	The preparation and phase transformation characteristics of Î ³ -Ti3O5 thin film. Journal of Materials Science: Materials in Electronics, 2017, 28, 7868-7873.	1.1	1
93	Tunable terahertz planar lens based on the dynamic meta-surface. , 2019, , .		1
94	Highly stable visibleâ€light photocatalytic properties of black rutile TiO2 hydrogenated in ultrafast flow. Journal of Materials Science: Materials in Electronics, 2021, 32, 14665-14676.	1.1	1
95	Ultrafast THz modulation characteristics of photo-induced metal-insulator transition of W-doped VO <inf>2</inf> film. , 2015, , .		0
96	Compare the phase transition properties of VO ₂ films from infrared to terahertz range. Phase Transitions, 2018, 91, 649-658.	0.6	0
97	λ-Ti <inf>3</inf> O <inf>5</inf> with Temperature and Laser Induced Phase Transition Characteristics for Active Tuning of Terahertz Wave Transmission. , 2018, , .		0